



# Energy and exergy analyses in convective drying process of multi-layered porous packed bed<sup>☆</sup>

Ratthasak Prommas, Pornthip Keangin, Phadungsak Rattanadecho<sup>\*</sup>

Research Center of Microwave Utilization in Engineering (R.C.M.E.), Faculty of Engineering, Thammasat University, Khlong Luang, Pathumthani, Thailand 12120

## ARTICLE INFO

Available online 9 July 2010

### Keywords:

Energy utilization  
Exergy efficiency  
Convective drying  
Multi-layered porous

## ABSTRACT

This paper is concerned with the investigation of the energy and exergy analyses in convective drying process of multi-layered porous media. The drying experiments were conducted to find the effects of multi-layered porous particle size and thermodynamics conditions on energy and exergy profiles. An energy analysis was performed to estimate the energy utilization by applying the first law of thermodynamics. An exergy analysis was performed to determine the exergy inlet, exergy outlet, exergy losses during the drying process by applying the second law of thermodynamics. The results show that the energy utilization ratio (EUR) and the exergy efficiency depend on the particle size as well as the hydrodynamic properties and the layered structure, by considering the interference between capillary flow and vapor diffusion in the multi-layered packed bed.

© 2010 Elsevier Ltd. All rights reserved.

## 1. Introduction

Drying is a thermal process in which heat and moisture transfer occur simultaneously. Heat is transferred by convection from heated air to the product to raise the temperatures of both the solid and moisture that is present. Moisture transfers occurs as the moisture travels to the evaporative surface of the product and then it evaporate into the circulating air as water vapor, are necessary for process design, optimization, energy integration, and control [1,2]. The heat and moisture transfer rates are therefore related to the velocity, temperature and type of product with the circulating drying air. Thermal drying has been recognized as an important unit operation as it is energy intensive and has a decisive effect on the quality of most products that are dried commercially [3,4].

Drying of porous solids is a subject of significant scientific and technological interest in a number of industrial applications including coatings, food, paper, textile, wood, ceramics, building materials, granular materials, electronic devices and pharmaceuticals [5].

Drying of porous materials is a problem of coupled heat and mass transport in a multiphase system which undergoes structural changes and shrinkage during the process. As drying proceeds, the mechanisms of water migration and all the transport properties change [6]. Nevertheless, most of the models describing the drying of foodstuffs are constructed on the basis of theories commonly used in dealing with

conventional porous materials, and without acknowledging the features which make this particular problem unusual.

The traditional thermodynamics method of assessing processes involving the physical or chemical processing of materials with accompanying transfer and transformation of energy is by the completion of an energy balance which is based on the first law of thermodynamics. The first law analysis is used to reduce heat losses or enhance heat recovery. Meanwhile, it gives no information on the degradation of the useful energy that occurs within the process equipment [7]. The exergy of an energy form or a substance is a measure of its usefulness or quality or potential change [8]. Exergy is defined as the maximum work, which can be produced by a system or a flow of matter or energy and it comes to equilibrium with a specified reference environment (dead state) [9]. Unlike energy, exergy is conserved only during ideal processes and destroyed due to irreversibilities in real processes [10].

The features of exergy are identified to highlight its importance in a wide range of applications [11]. Exergy analysis has been increasingly useful as a tool in the design, assessment, optimization and improvement of energy systems. It can be applied on both system and component levels. Exergy analysis leads to a better understanding of the influence of thermodynamics phenomena on effective process, comparison of the importance of different thermodynamics factors, and the determination of the most effective ways of improving the process [12]. As regards the exergy analyses of drying processes, some work has been carried out in recent years. Kanoglua and et al. [13] analyzed a thermodynamics aspect of the fluidized bed drying process of large particles for optimizing the input and output conditions by using energy and exergy models. The effects of the hydrodynamic and thermodynamics conditions were also analyzed such as inlet air

<sup>☆</sup> Communicated by W.J. Minkowycz.

<sup>\*</sup> Corresponding author.

E-mail address: [ratphadu@engr.tu.ac.th](mailto:ratphadu@engr.tu.ac.th) (P. Rattanadecho).

**Nomenclature**

$c_p$	specific heat, (kJ/kg K)
$\bar{c}_p$	mean specific heat, (kJ/kg K)
EUR	energy utilization ratio, (%)
Ex	exergy, (kJ/kg)
$g$	gravitational acceleration, $m/s^2$
$g_c$	constant in Newton's law
$h$	enthalpy, (kJ/kg)
$J$	joule constant
$\dot{m}$	mass flow rate, (kg/s)
$N$	number of species
$P$	pressure, (kPa)
$Q$	net heat, (kJ/s)
$Q_u$	useful energy given by heater, (kJ/s)
$s$	specific entropy, (kJ/kg K)
$T$	temperature, (K)
$u$	specific internal energy, (kJ/kg)
$v$	specific volume, $m^3/s$
$V$	velocity, (m/s)
$w$	specific humidity, (g/g)
$\dot{W}$	energy utilization, (J/s)
$z$	altitude coordinate, (m)

*Subscripts*

a	air
da	drying air
dc	drying chamber
f	fan
i	inlet
L	loss
mp	moisture of product
o	outlet
pb	porous packed bed
sat	saturated
$\infty$	surrounding or ambient

*Greek symbols*

$\phi$	relative humidity, (%)
$\eta_{ex}$	exergetic efficiency, (%)
$\mu$	chemical potential, (kJ/kg)

temperature, fluidization velocity and initial moisture content on energy efficiency and exergy efficiency. Syahrul and et al. [14] and Dincer [15] used a model to analyze exergy losses of a air drying process. Their work demonstrated that the usefulness of exergy analysis in thermodynamics assessments of drying processes and providence the performances and efficiencies of these processes. Akpinar and et al. [16,17] studied energy and exergy of the drying of red pepper slices in a convective type dryer, with potato slices in a cyclone type dryer and pumpkin slices in a cyclone type dryer. The type and magnitude of exergy losses during drying was calculated. Colak [18] performed an exergy analysis of thin layer drying of green olive in a tray dryer. In Colak's study the effects of the drying air temperature, the mass flow rate of drying air and olives on the system performance were discussed. Ceylan et al. [19] carried out energy and exergy analyses during the drying of two types of timber. The effects of ambient relative humidity and temperature were taken into account.

Typical applications of non-uniform material include The tertiary oil recovery process, geothermal analysis, asphalt concrete pavements

process and preservation process of food stuffs. Therefore, knowledge of heat and mass transfer that occurs during convective drying of porous materials is necessary to provide a basis for fundamental understanding of convective drying of non-uniform materials. From research on energy and exergy analysis of the drying process the analysis on the phenomenon of evaporation in porous materials is relatively small. Prommas [20] analyzed the energy and exergy in drying process of porous media using hot air. Due to the limited amount of experimental work on convective drying of multi-layered material, the various effects are not fully understood and a number of critical issues remain unresolved. The effects of particle size and the layered configuration on the overall drying kinetics have not been systematically studied. Although most previous investigations consider single-layered material, little effort has been reported on convective drying of multi-layered material (non-uniform structure) at a fundamental level.

From macroscopic point of view, the effects of the particle sizes, hydrodynamic properties, and the layered configuration on the overall drying kinetics must be clarified in detail. Therefore, the specific objectives of this work are to extend the previous work of Prommas to discuss the effect of particle size and the layered configuration on the overall drying kinetics include the convective drying of multi-layered porous packed bed.

The objectives of this work are described of multi-layered to effect of particle size and capillary pressure for evaluate the exergy losses of two operations multi-layered porous packed bed, the exergy losses and exergy input for the different drying operations and the influences of operating parameters on exergy losses. The knowledge gained will provide an understanding in multi-layered porous media and the parameters which can help to reduce energy consumptions and losses.

**2. Experimental apparatus**

Fig. 1(a) shows the experimental convective drying system. The hot air, generated electrically travels through a duct toward the upper surface of two samples situated inside the test section. The outside walls of test section are covered with insulation to reduce heat loss to the ambient. The flow outlet and temperature can be adjusted at a control panel.

As shown in Fig. 1(b), the samples are unsaturated packed beds composed of glass beads, water and air. The samples are prepared in the two configurations in the: a single-layered porous packed bed (uniform packed bed) with bed depth  $\delta = 40$  mm ( $d = 0.15$  mm (F bed) and  $d = 0.4$  mm (C bed)) and a two-layered porous packed bed, respectively. The two-layered porous packed bed are arranged in different configurations in the: F-C bed (fine particles ( $d = 0.15$  mm,  $\delta = 20$  mm) overlay the coarse particles ( $d = 0.4$  mm,  $\delta = 20$  mm)), and C-F bed (coarse particles ( $d = 0.4$  mm,  $\delta = 20$  mm) overlay the fine particles ( $d = 0.15$  mm,  $\delta = 20$  mm)), respectively. The width and total length of all samples used in the experiments are 25 mm and 40 mm, respectively. The temperature distributions within the sample are measured using fiberoptic sensors (LUXTRON Fluoroptic Thermometer, Model 790, accurate to 0.5), which are placed in the center of the sample at 5 mm from surface in Fig. 2. In each test run, the weight loss of the sample is measured using a high precision mass balance.

The uncertainty in the results might come from the variations in humidity and room temperature. The uncertainty in drying kinetics is assumed to result from errors in the measuring weight of the sample. The calculated uncertainties in weight in all tests are less than 2.8%. The uncertainty in temperature is assumed to result from errors in adjusting input power, ambient temperature and ambient humidity. The calculated uncertainty associated with temperature is less than 2.85%.

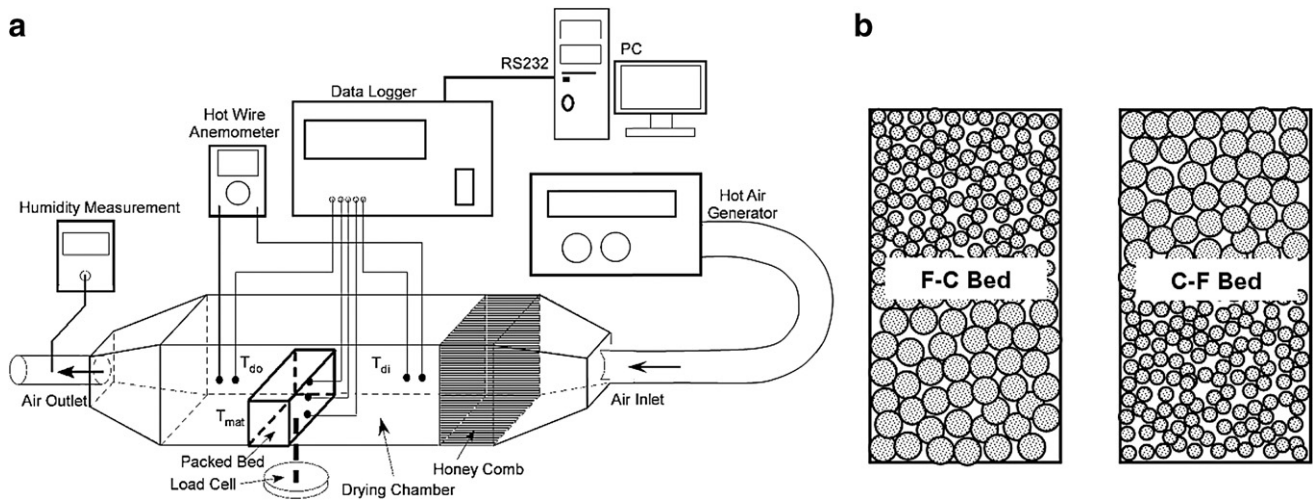


Fig. 1. Schematic of experimental facility: (a) Equipment setup; (b) Multi-layered porous packed bed (Sample).

### 3. The characteristic of moisture transport in multi-layered porous packed beds

As shown in Fig. 3 shows the typical multi-layered packed bed to be stated. The multi-layered packed beds are arranged in different configurations as follows:

- (a) F-C bed, the fine particles (average diameter of 0.15 mm) is over the coarse particles (average diameter of 0.4 mm).
- (b) C-F bed, the coarse particles (average diameter of 0.4 mm) is over the fine particles (average diameter of 0.15 mm).

It is observed that the moisture content profiles are not uniform in multi-layered packed beds. During convective drying, higher moisture content occurs in the fine bed while the moisture content inside coarse bed remains lower compared with the initial state. This is a result of capillary action.

From a macroscopic point of view, we will consider liquid water transport at the interface between two beds where the difference in particle size is considered. Fig. 4 shows typical moisture characteristic curve (relationship between capillary pressure ( $p_c$ ) and water saturation ( $s$ )) for the different particle sizes. In the case of the same capillary pressure, a smaller particle size corresponds to higher moisture content. Considering the case where two particle sizes having the same capillary pressure at the interface of different particle sizes are justified, as shown in Fig. 5. Since the capillary pressure has the same value at the interface between two beds the moisture content becomes discontinuous at the interface. This is a result of the differences in capillary pressure for the two particle layer. The physical and transport properties of the two sizes of particles composing the bed are shown in Table 1.

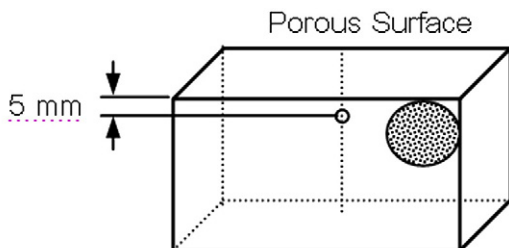


Fig. 2. The positions of temperature measurement in porous packed bed.

### 4. Mathematical formulation of problem

Schematic diagram of the convective drying model for multi-layered porous packed bed is shown in Fig. 6 [21]. When a porous packed bed is heated by hot air flowing over its upper surface, the heat is transferred from the top of porous packed bed into the interior. Therefore, the temperature gradient is formed in the bed, and the

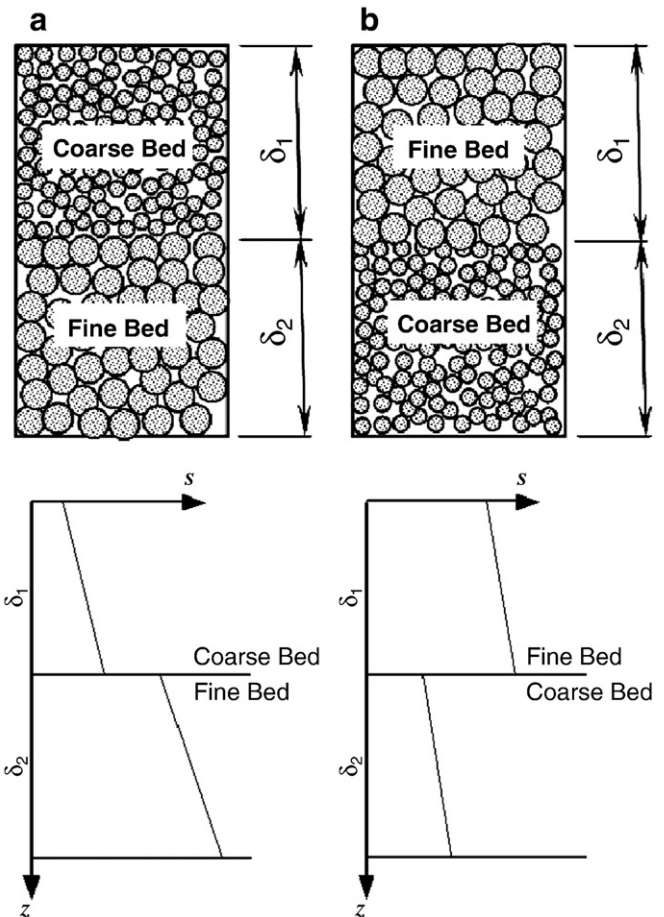


Fig. 3. Shows the typical profile of moisture content in multi-layered porous packed bed during convective drying in the cases of: (a) C-F bed (b) F-C bed.

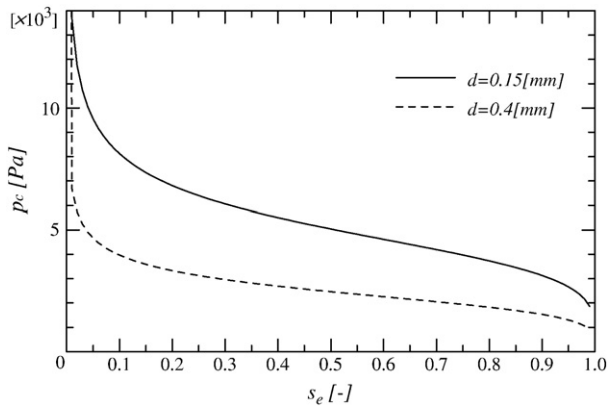


Fig. 4. Typical relationship between capillary pressure and water saturation [21].

liquid phase at the upper surface of porous packed bed evaporates by the variation of saturated vapor concentration corresponding to this temperature gradient as long as the surface remains wetted. In analysis, the main assumptions involved in the formulation of the transport model are:

1. The capillary porous material is rigid and no chemical reactions occur in the sample.
2. Local thermodynamics equilibrium is reached among each phase.
3. The gas phase is ideal in the thermodynamics sense.
4. The process can be modeled as steady-flow.
5. The multi-layered porous packed bed sample side wall is perfectly except the top surface insulated, hence adiabatic.
6. In a macroscopic sense, the porous packed bed is assumed to be homogeneous and isotropic, and liquid water is not bound to the solid matrix.

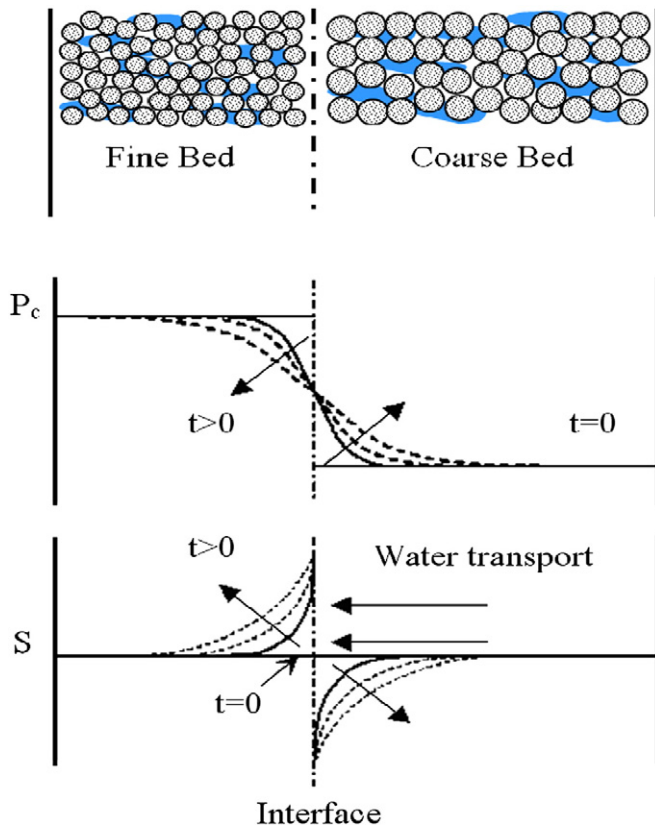


Fig. 5. Schematic diagram of water transport at the interface of multi-layered porous packed bed during convective drying process.

Table 1

The characteristic of water transport in porous packed bed [21].

Diameter, d (mm)	Porosity, $\phi$	Permeability, k (m <sup>2</sup> )
0.15	0.387	$8.41 \times 10^{-12}$
0.4	0.371	$3.52 \times 10^{-11}$

7. A dry layer (evaporation front) is formed immediately after water saturation approaches the irreducible value.
8. The volumes of the upper layer and lower layer are equal.
9. The distributions of water saturation in the layered porous packed beds differ greatly depending on the structure of layered porous packed beds even if the total volume of water that exists among the pores in the porous packed beds is identical.

By energy and exergy analyses in drying process of multi-layered porous packed bed using hot air, the main basic equations are given as follows:

#### 4.1. Energy analysis

A schematic diagram of the model is shown in Fig. 6. By applying the principle of conservation of mass and energy in the sample, the governing equation of mass and energy for all phases can be derived by using the volume average technique. The main transport mechanism describes moisture movement during drying by means of convection mode within the sample including liquid flow driven by capillary pressure gradient and gravity while the vapor is driven by the gradient of the partial pressure of the evaporating species. The traditional methods of thermal system analysis are based on the first law of thermodynamics. These methods use an energy balance on the control volume to determine heat transfer between the system and its environment. The first law of thermodynamics introduces the concept of energy conservation, which states that energy entering a thermal system with fuel, electricity, flowing streams of matter, and so on is conserved and cannot be destroyed. In general, energy balances provide no information on the quality or grades of energy crossing the thermal system boundary and no information about internal losses.

The drying process includes the process of heating, cooling and humidification. The process can be modeled as steady-flow processes by applying the steady-flow conservation of mass (for both dry air and moisture) and conservation of energy principles, General equation of mass conservation of drying air:

$$\sum \dot{m}_{ai} = \sum \dot{m}_{ao} \tag{1}$$

General equation of mass conservation of moisture:

$$\sum (\dot{m}_{wi} + \dot{m}_{mp}) = \sum \dot{m}_{wo}$$

or

$$\sum (\dot{m}_{ai} w_i + \dot{m}_{mp}) = \sum \dot{m}_{ai} w_o \tag{2}$$

General equation of energy conservation:

$$\dot{Q} - \dot{W} = \sum \dot{m}_o \left( h_o + \frac{V_o^2}{2} \right) - \sum \dot{m}_i \left( h_i + \frac{V_i^2}{2} \right) \tag{3}$$

where the changes in kinetic energy of the fan were taken into consideration while the potential and kinetic energy in other parts of the process were neglected. During the energy and exergy analyses of porous packed bed drying process, the following equations were used to compute the enthalpy of drying air.

$$h = c_{pda} T + w h_{sat@T} \tag{4}$$

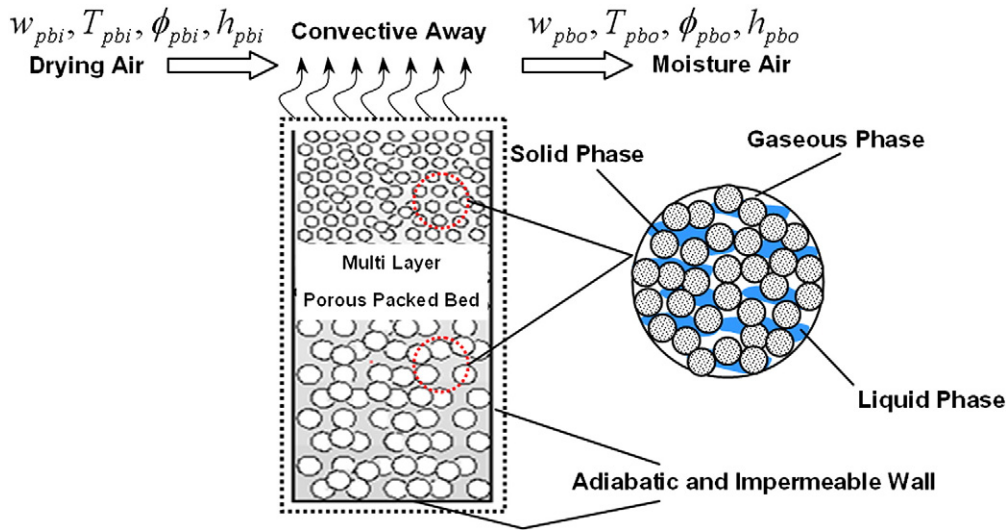


Fig. 6. Physical model of multi-layered porous packed bed.

The enthalpy equation of the fan outlet was obtained Bejan [22] using Eq. (5) as below:

$$h_{fo} = \left[ \left( \dot{W}_f - \frac{V_{fo}^2}{2 \cdot 1000} \right) \left( \frac{1}{\dot{m}_{da}} \right) \right] + h_{fi} \tag{5}$$

where,  $h_{fi}$  characterizes the enthalpy of drying air at the inlet of the fan,  $h_{fo}$  the enthalpy at the outlet of the fan,  $V_{fo}$  the drying air velocity at the outlet of the fan,  $\dot{W}_f$  fan energy and  $\dot{m}_{da}$  mass flow of drying air. Considering the values of dry bulb temperature and enthalpy from Eq. (5), the specific and relative humidity of drying air at the outlet of the fan were determined Akpinar [16]. The inlet conditions of the heater were assumed to be equal to the outlet conditions of the fan. The useful energy gained from the heater enters the drying chamber as the convection heat source, which was defined as:

$$\dot{Q}_u = \dot{m}_{da} C_{pda} (T_{ho} - T_{hi}) \tag{6}$$

where  $T_{ho}$ ,  $T_{hi}$  are the outlet and inlet temperature of air at the heating section. The inlet conditions of the drying chamber were determined depending on the inlet temperatures and specific humidity of drying air. It was considered that the mass flow rate of drying air was equally passed throughout the chamber. The specific humidity at the outlet of the chamber can be defined as:

$$w_{pbo} = w_{pbi} + \frac{\dot{m}_{wpcb}}{\dot{m}_{da}} \tag{7}$$

where,  $w_{pbi}$  denotes the specific humidity at the inlet of the porous packed bed chamber,  $\dot{m}_{wpcb}$  the mass flow rate of the moisture removed from porous packed bed samples. The heat utilized during the humidification process at the chamber, can be estimated by

$$\dot{Q}_{pb} = \dot{m}_{da} (h_{pbi@T} - h_{pbo@T}) \tag{8}$$

where,  $h_{pbi@T}$  and  $h_{pbo@T}$  identify orderly the enthalpies at the inlet and outlet of porous packed bed chamber. The enthalpy of moisture air outlet of porous packed bed chamber can be defined as:

$$h_{pbo@T} = h_{pbi@T} - w_{pbo} h_{sat@T} \tag{9}$$

where  $w_{pbo}$  is the amount of product moisture evaporated. The energy utilization ratio for the drying chamber can be obtained using the following expression Akpinar [16]:

$$EUR_{dc} = \frac{\dot{m}_{da} (h_{pbi@T} - h_{pbo@T})}{\dot{m}_{da} C_{pda} (T_{ho} - T_{hi})} \tag{10}$$

#### 4.2. Exergy analysis

The second law of thermodynamics introduces the useful concept of exergy in the analysis of thermal systems is show in Fig. 6. As known, exergy analysis evaluates the available energy at different points in a system. Exergy is a measurement of the quality or grade of energy and it can be destroyed in the thermal system. The second law states that part of the exergy entering a thermal system with fuel, electricity, flowing streams of matter, or other sources is destroyed within the system due to irreversibilities. The second law of thermodynamics uses an exergy balance for the analysis and the design of thermal systems. In the scope of the second law analysis of thermodynamics, total exergy of inflow, outflow and losses of the drying chamber are estimated. The basic procedure for exergy analysis of the chamber is determined the exergy values at steady-state points and the reason of exergy variation for the process. The exergy values are calculated by using the characteristics of the working medium from a first law energy balance. For this purpose, the mathematical formulations used to carry out the exergy balance are as show below Ahern [23].

$$\begin{aligned} \text{Exergy} = & (u - u_\infty) - T_\infty (s - s_\infty) + \frac{P_\infty}{J} (v - v_\infty) + \frac{V^2}{2gJ} + (z - z_\infty) \frac{g}{g_c J} \\ & \text{internal entropy} \quad \text{work} \quad \text{momentum} \quad \text{gravity} \\ & \text{energy} \\ & + \sum_c (\mu_c - \mu_\infty) N_c + E_i A_i F_i (3T^4 - T_\infty^4 - 4T_\infty T^3) + \dots \tag{11} \\ & \text{chemical} \quad \text{radiation} \quad \text{emission} \end{aligned}$$

The subscript  $\infty$  denotes the reference conditions. In the exergy analyses of many systems, only some of the terms shown in Eq. (11) are used but not all. Since exergy is energy available from any source, it can be developed using electrical current flow, magnetic fields, and

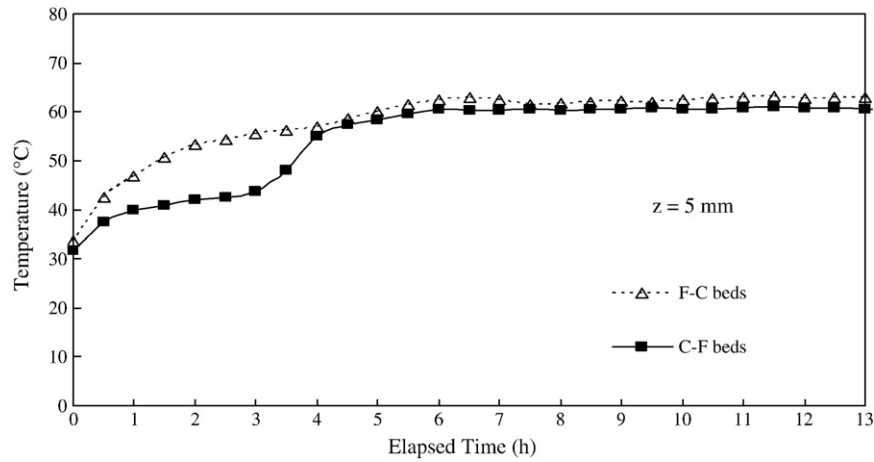


Fig. 7. The variation of temperature profiles with respect to time.

diffusion flow of materials. One common simplification is to substitute enthalpy for the internal energy and  $PV$  terms that are applicable for steady-flow systems. Eq. (11) is often used under conditions where the gravitational and momentum terms are neglected. In addition to these, the pressure changes in the system are also neglected because of  $v \approx v_\infty$ , hence Eq. (11) is reduced as:

$$Exergy = \bar{c}_p \left[ (T - T_\infty) - T_\infty \ln \frac{T}{T_\infty} \right] \quad (12)$$

The inflow and outflow of exergy can be found using the above expression depending on the inlet and outlet temperatures of the drying chamber. Hence, the exergy loss is determined as:

$$Exergy\ loss = Exergy\ inflow - Exergy\ outflow$$

$$\sum Ex_L = \sum Ex_i - \sum Ex_o \quad (13)$$

The exergy inflow for the chamber is stated as below

$$Ex_{dci} = Ex_{pbi} = \bar{c}_{pda} \left[ (T_{dci} - T_\infty) - T_\infty \ln \frac{T_{dci}}{T_\infty} \right] \quad (14)$$

The exergy outflow for the drying chamber is stated as:

$$Ex_{dco} = Ex_{pbo} = \bar{c}_{pda} \left[ (T_{dco} - T_\infty) - T_\infty \ln \frac{T_{dco}}{T_\infty} \right] \quad (15)$$

The exergetic efficiency can be defined as the ratio of the product exergy to exergy inflow for the chamber as outlined below:

$$Exergy\ Efficiency = \frac{Exergy\ inflow - Exergy\ loss}{Exergy\ inflow} \quad (16)$$

$$\eta_{Ex} = 1 - \frac{Ex_L}{Ex_i} \quad (17)$$

### 5. Results and discussion

Fig. 7 shows the measured temperature profiles within the multi-layered porous packed beds for  $s_0 = 0.5$ ,  $T_a = 70^\circ\text{C}$ ,  $U_\infty = 1.2$  (m/s) and bed depth ( $z$ ) at a level of 5 mm in cases of F-C and C-F beds as a function of elapsed time. The physical properties are given in Table 1. It can be observed that at the early stage of the drying process the temperature increase in both cases are nearly the same profiles. It is well-known that the temperature increases as drying progresses. This is because the latent heat transfer in evaporation process is retained due to the decline of the mass transfer rate together with the decreases of average moisture content. Nevertheless the temperature profile of the F-C bed increases with a higher rate than the C-F bed. This is because the dry layer formed earlier in the F-C bed and abrupt temperature rise occurs as the dry bulb temperature is approached. On the other hand, in the case of the C-F bed the temperature slowly increases in comparison with the F-C bed due to the late formation of

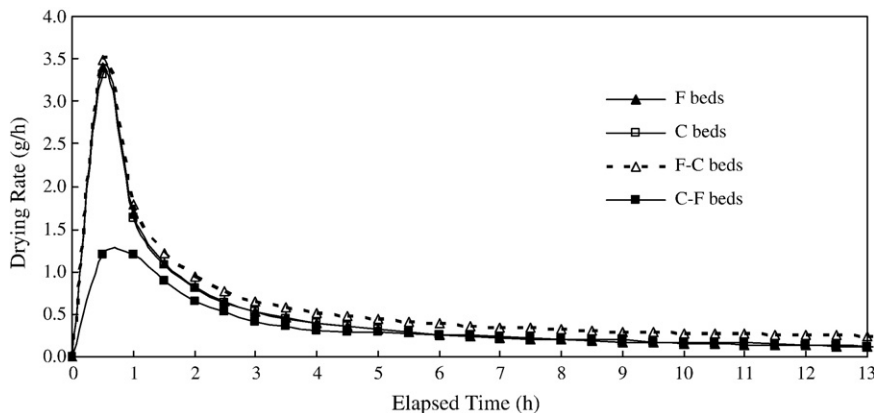


Fig. 8. The variation of drying rate with respect to time.

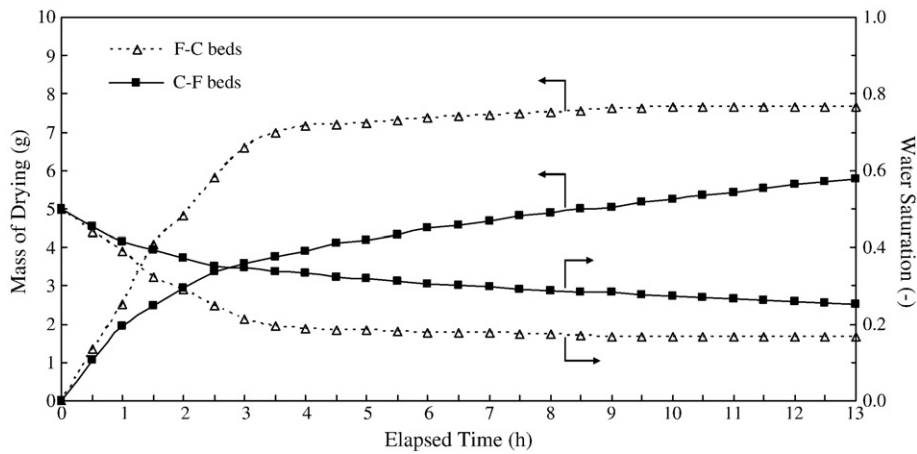


Fig. 9. The variation of water saturation and mass of drying in multi-layered porous packed bed with respect to time.

dry layer. In this regime [21], the liquid flows due to the gradient in the capillary pressure, and gravity can induce this flow. In addition, the presence of temperature gradient within the medium and the consecutive existence of surface tension gradient move the liquid away from the heated surface (opposing the capillary effect). Thus, capillarity, gravity, and thermo-capillarity flow are the most significant forces governing the liquid motion [24]. As the liquid flows out of the medium, the local saturation throughout the sample decreases with increasing heating time, where the saturation at the heated permeable surface decreased faster (because the liquid flow towards the lowest saturation and also the resistance to liquid flow increases with decreasing in saturation thus requiring large saturation gradients). At the end of the funicular regime the surface saturation drops to the irreducible saturation. The time at which this occurs is called the critical time. For a short period after heating, the heated surface will be intermittently dry. This is associated with a decrease in the drying rate. After this intermittent surface-drying period, the moving interface regime begins. The surface becomes completely dry, the surface temperature increases rapidly, and the heat transferred to the porous medium results in penetration of the evaporation front (a moving interface) into the medium.

At the longer drying time, the temperature profile at any instant tends to be constant shape throughout the region. In this period, the vapor diffusion effect plays an important role in the moisture migration mechanism because of the sustained vaporization that is generated within the sample. The vapor is superheated in the dry region (temperature distribution in the dry region is shown in Fig. 7) and in equilibrium with the liquid in the wet region. As the elapsed

time increases, the total pressure in the wet region increases indicating significant bulk evaporation as a consequence of a rise in the temperature of the wet region.

Figs. 8 and 9 show the variations of drying mass and drying rate with respect to time for the two packed packed beds (F-C and C-F beds). It is observed that the variations of drying mass and drying rate and temperature are interrelated. The drying speed is greatly different although the initial water saturation is the same. The F-C bed dries faster than C-F bed. This is due to the difference in the moisture content in the neighborhood of the drying surface. Since the driving force of heat and mass transfer is very large when moisture content and temperature in neighborhood of the drying surface is high. Consequently, the drying is very fast in case of F-C bed.

In the microscopic sense, the drying rate rises quickly in the early stages of drying (which corresponds to higher moisture content at the upper surface) and then decreases and reaches a plateau before decreasing again when the formation of a drying front is established. It is evident from the figure that the increase in drying rate can become significant when the F-C bed is utilized. This is a result of the strong effect of capillary pressure in F-C bed. For this case the capillary pressure easily overcomes the resistance caused by the lower permeability and maintains a supply of liquid water near the surface.

In the case of two-layered packed beds (F-C bed and C-F bed), the moisture content profiles become discontinuous at the interface between the two layers, namely, the moisture content in the upper layer is higher than that for the lower layer in F-C bed, while the moisture content in the upper layer is lower than that for the C-F bed. This is because the equilibrium water saturation under the same

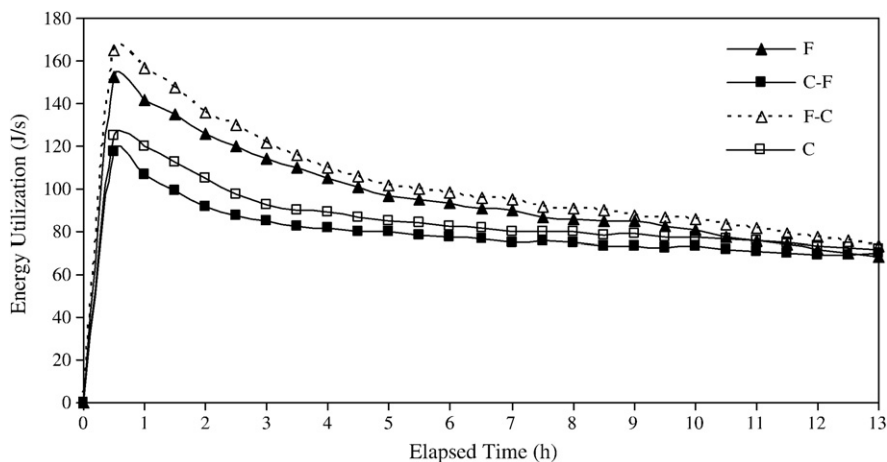


Fig. 10. Variation of energy utilization and drying time with different porous packed bed.

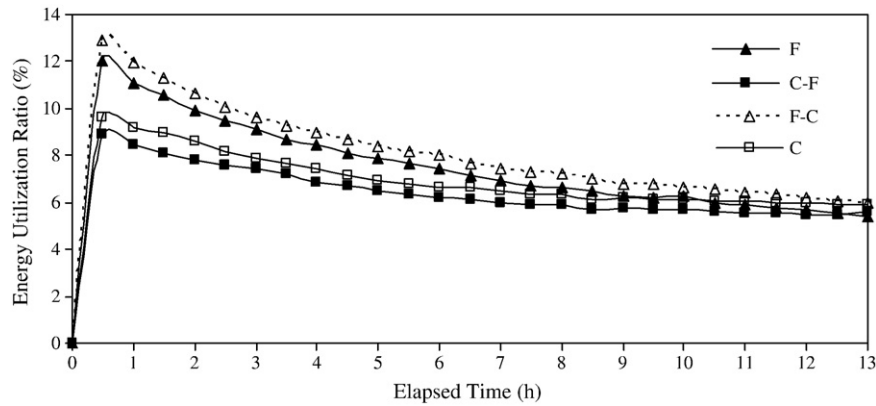


Fig. 11. Variation of energy utilization ratio with different porous packed bed.

capillary pressure differs according to the particle sizes smallest particle size corresponding to higher water saturation. Therefore, the drying kinetics is strongly influenced by the difference in water saturation. Continuing the drying process (Fig. 9) causes the average water saturation inside the F–C bed to decrease quickly in comparison with the C–F bed. In the case of the C–F bed, in contrast to that F–C bed, the moisture content in the upper layer (C bed) is very low and the dry layer is formed rapidly while the moisture content in the lower layer (F bed) remains high. This is due to the C bed (which corresponds to a lower capillary pressure) located above the F bed retards the upward migration of liquid water through the interface between two layers and also due to the effect of gravity.

According to the experimental results from Figs. 7–9, these results can be used as the input parameters for analyzing the energy utilization (Eqs. (8) to (10)) and exergy efficiency (Eqs. (11) to (17)) as follows:

Fig. 10 shows the variation of energy utilization as a function of drying time of different configurations and drying time. The energy utilization is relatively high at the beginning of drying process due to the high moisture content of the sample, and consequently gradually decrease because the low moisture content of the samples at the end of the process.

Fig. 11 shows the variation of energy utilization ratio against drying time of F–C and C–F packed bed. Energy balance is analyzed to evaluate the energy utilization ratio. The values of energy utilization ratio in drying chamber are calculated by using Eq. (10). When velocity and the temperature of hot air are kept constantly, the energy utilization ratio values are seem to be similar to energy utilization due to energy inlet of drying process to be constant.

In order to calculate the exergetic efficiency of the drying process, exergy analysis is taken into consideration. The exergy inflow rates

were calculated by using Eq. (14) as function of the ambient and inlet temperatures. The exergy inflow during the drying of multi-layered porous packed bed is attracted by drying layered of porous packed bed. The exergy outflows are calculated by using Eq. (15) and during the experiments which varied. It was observed that the exergy outflow from the drying chamber slowly increases with an increase of the drying time.

The exergetic efficiency of the drying chamber increases with an increase of drying time as shown in Fig. 12. The variation of exergy efficiency with respect to time is inversely with energy utilization ratio. This is because during drying process the available energy in the drying chamber increases as an increase of drying time, since moisture content decreases with time. The effect of the multi-layered on the drying time as well as the exergy efficiency of the drying system is also presented. The exergy efficiencies in case of C–F bed are higher than that of the F–C bed approximate 10% after 1 h of drying time thought the drying process. The results show that the energy utilization and exergy efficiency in Figs. 10–12 are strongly depended of layered configuration and particle size as described in Figs. 1–9.

## 6. Conclusion

The experimental analysis presented in this paper describes many important interactions within multi-layered porous materials during convective drying. The following paragraph summarizes the conclusions of this study:

The effects of particle sizes and layered configuration on the overall drying kinetics are clarified. The drying rate in the F–C bed is slightly higher than that of the C–F bed. This is because the higher capillary pressure for the F–C bed results in to maintain a wetted drying surface for a longer period of time. The F–C bed displays the

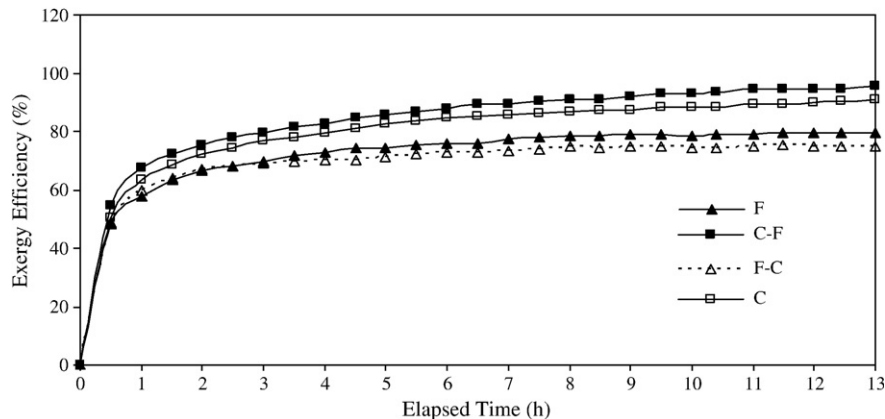


Fig. 12. Variation of exergy efficiency with different porous packed bed.

drying curve which differentiates it from the others. It has a shorter drying time due to the strong effect of capillary action.

Energy and exergy of the drying process of the multi-layered porous packed bed were analyzed. It can be concluded that energy utilization, energy utilization ratio and exergy efficiency strongly depend on particle size and multi-layered configurations

### Acknowledgment

The authors would like to express their appreciation to the Commission on Higher Education, Thailand and Thailand Research Fund (TRF) for providing financial support for this study.

### References

- [1] I. Dincer, M.A. Rosen, Energy, environmental and sustainable development, *Applied Energy* 46 (1999) 427–440.
- [2] I. Dincer, A.Z. Sahin, Incorporation of the dincer number into the moisture diffusion equation, *International Communications in Heat and Mass Transfer* 3 (2004) 109–119.
- [3] A.S. Mujumdar, An overview of innovation in industrial drying: current status and R&D needs, *Transport in Porous Media* 66 (2007) 3–18.
- [4] I. Białobrzeski, M. Zielińska, A.S. Mujumdar, M. Markowski, Heat and mass transfer during drying of a bed of shrinking particles – simulation for carrot cubes dried in a spout-fluidized-bed drier, *International Journal of Heat and Mass Transfer* 51 (2008) 4704–4716.
- [5] N.M. Panagiotou, A.K. Stubos, G. Bamopoulos, Z.B. Maroulis, Kinetics of a multi-component mixture of organic solvents, *Drying Technology* 17 (1999) 2107–2122.
- [6] A.G. Yiotis, A.K. Stubos, A.G. Boudouvis, Y.C. Yortsos, A 2-D pore-network model of the drying of single-component liquids in porous media, *Advances in Water Resources* 24 (2001) 439–460.
- [7] R.G. Carbonell, S. Whitaker, Dispersion in pulsed systems – II Theoretical developments for passive dispersion in porous, *Chemical Engineering Science* 38 (1983) 1795–1802.
- [8] T. Tekcin, M. Bayramoglu, Exergy loss minimization analysis of sugar production process from sugar beet, *Food and Bioproducts Processing* 76 (1998) 149–154.
- [9] M.A. Rosen, I. Dincer, On exergy and environmental impact, *International Journal of Energy Research* 21 (1998) 643–654.
- [10] M.A. Rosen, D.S. Scott, Entropy production and exergy destruction: Part I – hierarchy of earth's major constituencies, *International Journal Hydrogen Energy* 28 (2003) 1307–1313.
- [11] A.I. Liapis, R. Bruttini, Exergy analysis of freeze drying of pharmaceuticals in vials on trays, *International Journal of Heat and Mass Transfer* 51 (2008) 3854–3868.
- [12] Y. Liu, Y. Zhao, X. Feng, Exergy analysis for a freeze-drying process, *Applied Thermal Engineering* 28 (2008) 675–690.
- [13] M. Kanoglua, I. Dincer, M.A. Rosen, Understanding energy and exergy efficiencies for improved energy management in power plants, *Energy Policy* 35 (2007) 3967–3978.
- [14] S. Syahrul, I. Dincer, F. Hamdullahpur, Thermodynamics modeling of fluidized bed drying of moist particles, *International Journal of Thermal Sciences* 42 (2003) 691–701.
- [15] I. Dincer, A.Z. Sahin, A new model for thermodynamics analysis of a drying process, *International Journal of Heat and Mass Transfer* 47 (2004) 645–652.
- [16] E.K. Akpınar, Energy and exergy analyses of drying of red pepper slices in a convective type dryer, *International Communication in Heat and Mass Transfer* 31 (2004) 1165–1176.
- [17] E.K. Akpınar, A. Midilli, Y. Bicer, Energy and exergy of potato drying process via cyclone type dryer, *Energy Conversion and Management* 46 (2005) 2530–2552.
- [18] N. Colak, A. Hepbasli, Performance analysis of drying of green olive in a tray dryer, *Journal of Food Engineering* 80 (2007) 1188–1193.
- [19] I. Ceylan, M. Aktas, H. Dogan, Energy and exergy analysis of timber dryer assisted heat pump, *Applied Thermal Engineering* 27 (2007) 216–222.
- [20] R. Prommas, P. Rattanadecho, D. Cholaseuk, Energy and exergy analyses in drying process of porous media using hot air, *International Communications in Heat and Mass Transfer* 37 (2010) 372–378.
- [21] P. Rattanadecho, K. Aoki, M. Akahori, Experimental and numerical study of microwave drying in unsaturated porous material, *International Communications in Heat and Mass Transfer* 28 (2001) 605–616.
- [22] A. Bejan, *Advanced Engineering Thermodynamics*, John Wiley and Sons, New York, 1998.
- [23] J.E. Ahern, *The Exergy Method of Energy Systems Analysis*, John Wiley, New York, 1980.
- [24] M. Kaviani, J. Rogers, Funicular and evaporative-front regimes in convective drying of granular beds, *International Journal of Heat and Mass Transfer* 35 (1992) 469–480.